The International Journal of Engineering and Information Technology

journal homepage:www.ijeit.misuratau.edu.ly

Theoretical and Experimental Investigation of Liquid and Gas Flow Pressure Drop through Different Sections of A Partially Closed Piping system

Mahmoud O. Elsharafi
McCoy School of Engineering, Midwestern State University
Wichita Falls, TX, USA.

Christopher J. Alexis
McCoy School of Engineering, Midwestern State University
Wichita Falls, TX, USA.

Trevon Antoine
McCoy School of Engineering, Midwestern State University
Wichita Falls, TX, USA.

Mohamed M. Ahmed
Petroleum Engineering Dept., Collage of Engineering, Sirte University,
Sirte, Libya

Abdunaser O. Susi
Petroleum Engineering Dept., Collage of Engineering, Misurata University
Misurata, Libya

Abstract— **Multiphase flow is found in various places in nature and practice. However, multiphase flow is prevalent in the petroleum production industry. This phenomenon gives rise to a significant issue of pressure loss within piping systems, resulting in a loss in production. Multiphase flow has been studied for decades; however, with the increase in unconventional engineering methods, there is now a greater need for its study. This study investigates phenomena related to multiphase flow, such as flow regimes and pressure loss produced by friction, pipe orientation, and various fluid phase properties. An experimental system was designed, and different fluid phases were used to represent varying situations in piping systems. The system included sections of horizontal, inclined, and vertical pipe orientations experienced during hydrocarbon migration from the reservoir to the surface. To replicate industry multiphase flow in the experimental system, we used water to represent the oil and compressed air to represent gas. The pressure differences throughout the system were calculated using the Beggs and Brill Correlation, the Lockhart-Martinelli Parameter, and the Chisholm Equation. Experimental pressure differences and the effect of the choke valve positions were also recorded for the different sections of the system while observing the flow regimes produced by multiphase fluid interaction. Through the research methods, we found that most pressure losses occurred in the elbows, and most frictional pressure loss occurred in the vertical 3ft pipe, while the 45° and 90° downhill pipes experienced increased pressure.**

Index Terms: **Multiphase flow, Two-phase flow, Pressure drop, Flow regime, Piping systems.**

I. INTRODUCTION

The term multiphase flow or two-phase flow refers to the simultaneous flow of more than one fluid phase or component through a porous medium (Sun, B. 2016). There are three natural phases of materials: solid, liquid, and vapor or gas (Michaelides & Feng, 2016, p. 1). Hence, multiphase flow is found in various places in nature and practice. However, multiphase flow is prevalent in the petroleum production industry, where its significance is great since its comprehension can offer significant economic savings (Bai & Bai, 2012, p. 371). In nature, multiphase flow is found in various natural phenomena such as different forms of precipitation, namely rain and snow, and sediment transportation such as avalanches and landslides. In industry, multiphase flow occurs in oil and gas wells, gathering systems, and many other piping systems where fluids are transported from one location to another. The effective transportation of fluids is vital to human productivity, where pipes of a circular cross-sectional area are most frequently used in piping systems due to their structural advantage compared to any other shape. Specifically, circular pipes are used both in the subsurface and at the surface in the oil and gas industry. Circular pipes can withstand varying pressure differences between internal and external pressures without worrying about deformation. This structural advantage is significant in the subsurface, where internal and external pressures are generally higher than those experienced at the surface (Okoye 2016).

During production, crude oil is usually a mixture of gas, oil, and water or brine, which means multiphase flow to the surface is generally unavoidable (Sun, B. 2016). The simultaneous migration of multiple fluid phases in the wellbore produces a significant issue in the petroleum industry characterized as pressure loss. Pressure is essential during petroleum production as it determines the quantity and rate of hydrocarbons that can be retrieved from the subsurface to be refined at the surface and subsequently used as energy and other petroleum products. The

Received 20 Mar, 2022; revised 21 July, 2022; accepted 16 Aug, 2022.

Available online 20 Aug , 2022.

importance of pressure is related to three critical phases of petroleum production over a well's lifespan known as primary, secondary, and tertiary or enhanced oil recovery. The percentage of original oil defines these three phases in place retrieved or recovered from the reservoir and the methods used for oil recovery. (Alagorni, Abubaker H., et al., 2015).

With decades of experience in traditional oilwells, there are well-established methods to combat multiphase flow fluid problems in those wells. However, the increase in unconventional wells and the decrease in conventional oil production relative to unconventional production give rise to new issues relating to multiphase flow, such as underbalanced drilling, well control for kicking, acidic gas wells, and the well control for deep-water drilling making theoretical multiphase flow studies increasingly crucial in the 21st century (Sun, B. 2016).

The interaction of multiple fluid phases produces different fluid flow patterns known as flow regimes. These regimes are functions of operating conditions, fluid properties, flow rates, pipe orientation, and geometry (Corneliussen et al., 2005). Imagining multiphase flow behavior in an untested system without imagining how the phases are arranged given different parameters can be very difficult. Flow regime maps predict different flow patterns by correlating the parameters, such as their velocity. (Griffith, P. 1984). However, determining flow regimes in operating piping systems is generally tricky hence the importance of laboratory experiments to better understand flow regimes. In the laboratory, multiphase flow regimes can be studied through transparent piping by direct visual observation and subsequent characterization. The functions of flow regimes created by multiphase flow produce more concepts or phenomena that clarify the factors influencing pressure differences within piping systems. As multiphase flow occurs through a pipe, the volume of the pipe occupied by a single phase is often different from its proportion of the total volumetric flow rate due to the density differences between the different phases occupied by the pipe. In an upward flow, being inclined or vertical, the density difference between fluid phases causes the dense phase to "slip down" or be "held up" since the lighter phase moves faster through the pipe than the denser phase. As a result, the in-situ volume fraction of the more viscous phase will be greater than the input volume fraction. This also means the in-situ volume fraction of the lighter will be less than its input volume fraction phase (Sarah et al., 2014, p. 4946). This concept is known as liquid "hold-up," where its valve can be quantitively determined using correlation methods produced by previous experimental research.

Due to the complexity of multiphase flow, accurately predicting pressure loss in piping systems has proven difficult. This problem has given rise to many specialized solutions for limited multiphase flow conditions without any single explanation accepted for general operating conditions. This again creates a great need for the study of multiphase flow. In addition, for any pipe segment, the liquid velocity along the pipe wall can vary over short distances without any significant change in fluid property or pipe orientation. This result in variable frictional pressure loss due to liquid throughout any piping system with multiphase flow. During other conditions, which flow regimes can represent, the liquid phase can be almost wholly entertained in the gas phase, where the gas is represented by a film around the pipe's walls and the liquid within the core of the multiphase. This result in the liquid phase having very little influence on frictional pressure loss for that specific situation (Orkiszewski, 1967).

Since the 1960s, multiphase flow has been studied extensively and is becoming increasingly popular due to its relevance to the petroleum industry with the increase in unconventional engineering processes. Early research from Fancher and Brown, Duns and Ros, Hagedorn and Brown, Beggs and Brill, Stuhmiller, Taitel and Dukler, and Zhang and Prosperetti paved the way for today's multiphase flow correlations. Fancher & Brown (1963), who developed a no-slip correlation based on Poettmann and Carpenter's (1952) findings, can be used for any flow pattern. However, the correlation wasn't developed with a flow regime map (Fancher and Brown, 1963). During the same year, 1963, Duns and Ros experimented with nearly 4000 different multiphase tests with approximately 20,000 data points to calculate the pressure gradient with liquid hold-up using vertical flow in pipes ranging from 1.26 to 5.60 inches in diameter. From their experiments, Duns and Ros produced the flow regime map shown in figure 1.

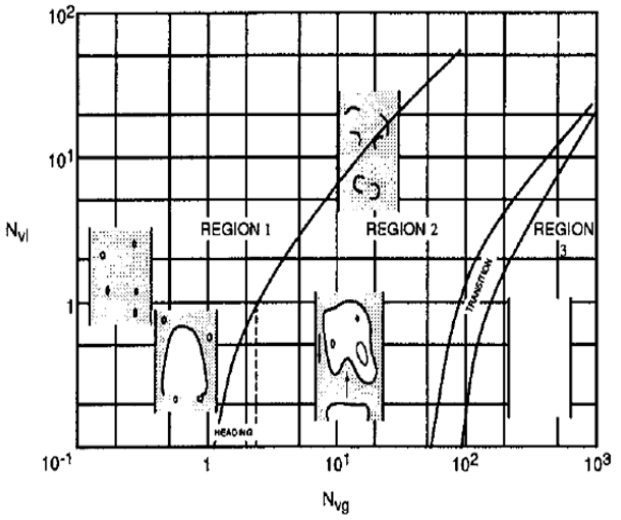

Figure 1. Duns and Ros Flow Regime Map (Duns and Ross, 1963)

Later, Hagedorn and Brown (1965) published an empirical two-phase flow correlation that doesn't distinguish between the flow regimes. However, they developed this correlation from 475 tests in a 1,500-foot experimental well, using fluids with viscosities up to 110 centipoises and through 1 inch, 1¼ inch, and 1½ inch nominal size tubing. They found no change to hold-up with deviation (Hagedorn and Brown, 1965). Following Hagedorn and Brown, Beggs and Brill developed a correlation by experimental study of a two-phase flow in horizontal and inclined pipes. They designed a system of 1-

inch and 1 ½-inch smooth circular pipes to investigate the inclination effect on liquid hold-up and pressure loss in gas and liquid two-phase flow (Beggs and Brill, 1973). Then, Stuhmiller studied the influence of interfacial pressure forces on the character of two-phase flow model equations in 1977. In addition, Zhang and Prosperetti found that phase interactions also result in stress in a potential flow (Zhang and Prosperetti, 1997). Taitel and Dukler (1980) introduced referring to the description of the simultaneous flow of gas and liquid in vertical pipes, with names such as bubble, slug, and annular flow. Their results are shown in the form of a cross plot with the superficial gas velocity (vgs), on the x-axis and the superficial liquid velocity (vls), on the y-axis, which is shown in figure 2 (Taitel et al., 1980).

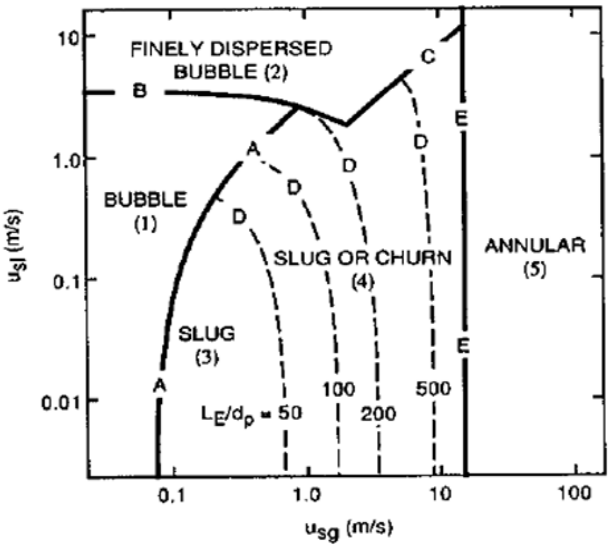

Figure 2: Taitel and Dukler Flow Regime Map (Taitel et al., 1980)

Today, there are numerous well-defined flow regimes such as bubble, slug, plug, churn, annular, stratified, stratified wavy, and mist flows (figure 3), building on the previous research by the researchers previously mentioned. However, these flow regimes can be grouped into three main categories: segregated or separated, intermittent, and dispersed (Corneliussen et al., 2005). Corneliussen et al., (2005) described that segregated or separated flow is characterized by a non-continuous phase distribution in the radial direction and a continuous phase in the axial direction of the pipe, where flows such as stratified and annular flow fall under this category. In addition, Corneliussen et al., (2005) characterized intermittent flow as being non-continuous in the axial direction, resulting in locally inconsistent behavior. Flows such as elongated bubble, churn, plug, and slug flow are categorized as intermittent flow. Corneliussen et al., (2005) further characterized dispersed flow as where uniform phase distributions are both in the radial and axial directions of the pipe where flows such as bubble and mist flow fall under this category, as shown in figure 3.

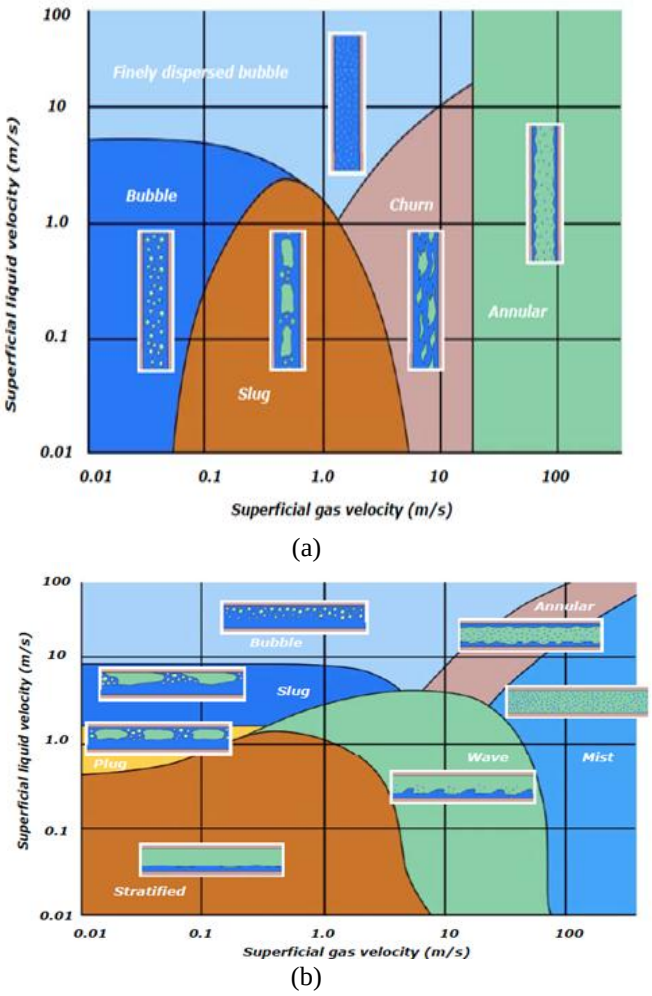

Figure 3: Flow Regime Maps a) Multiphase Flow in Vertical Pipes) b) Multiphase Flow in Horizontal Pipes (Corneliussen et al., 2005)

II. THEORY

To calculate pressure losses within our system, we had to find accurate and well established models. We evaluated various methods used from 1949, such as the Lockhart-Martinelli (1949), Fancher & Brown (1963), Duns and Ros (1963), Hagedorn and Brown (1965), and Beggs & Brill (1973). After extensive evaluation and careful consideration, we decided the Lockhart-Martinelli (1949) and Beggs & Brill (1973) would yield the most accurate results given our system and parameters. The Beggs & Brill correlation is used to calculate the pressure drop in the vertical and inclined sections present in our system, which requires the knowledge of the different flow patterns present in the pipes as well as liquid velocity number and Froude's number.

The Lockhart-Martinelli parameter is used to calculate the two-phase pressure drop in the horizontal sections of the system. This parameter was first introduced by Lockhart-Martinelli (1949) and is defined as the square root of the ratio of the pressure gradient of liquid to the pressure

by the gradient of gas or vapor. As such, the pressure gradient of both phases (liquid and air) has to be calculated separately (Kutty et al., 2017). After the pressure gradient is found for each phase, the Chisholm (1967) equations are used as multipliers to combine both pressure gradients, which yield the total pressure loss of the horizontal section of the piping system.

III. HORIZONTAL PIPE ORIENTATION (LOCKHART-MARTINELLI PARAMETER& CHISHOLM EQUATION)

3.1 Pressure Gradient Calculations

For this research, one of the main concerns was the determination of pressure losses experienced throughout the experimental system. As mentioned, the Lockhart-Martinelli method and the Chisholm Equation were used to calculate the pressure losses in our horizontal sections. The following steps were used to find our experimental system's total multiphase pressure gradient for horizontal sections.

To find the pressure gradient, the cross-sectional area, A_c is determined by the following formula:

$$A_c = {D_H}^2 \quad \text{..... (1)}$$

The Mass Flux, j can then be calculated

$$j = \frac{\dot{m}}{A_c} \quad \text{..... (2)}$$

Once Mass Flux is calculated, the Reynolds number, R_{H2O} is determined

$$R_{H2O} = \frac{j * D_H}{\mu}, \quad \text{..... (3)}$$

Find friction factor, f_{H2O} is also calculated from Reynolds number

$${f_{H2O}}^{-0.5} = -1.8 log_{10}\left(\left(\frac{\frac{e}{D}}{3.7 D_H}^{1.11}\right) + \left(\frac{6.9}{R_{H2O}}\right)\right) \text{..... (4)}$$

Lastly, the pressure gradient, $(\Delta P/L)\ H_2O$ is calculated

$$\left(\frac{\Delta P}{L}\right)_{H2O} = \frac{f_{H2O} * (j_{H2O})^2}{2 * \rho_{H2O} * D_H} \quad \text{..... (5)}$$

The steps above are then repeated to find the pressure gradient for air using equations 1 – 5.

Lockhart-Martinelli Parameter

From the Pressure Gradient ($\frac{\Delta P}{L}$), the Lockhart-Martinelli parameter, X is given by:

$$X = \sqrt{\frac{\left(\frac{\Delta P}{L}\right)_{H2O}}{\left(\frac{\Delta P}{L}\right)_{air}}} \quad \text{..... (6)}$$

3.2 Total Multiphase Pressure Gradient

First, the Water Pressure Gradient Multiplier (Chisholm Equation), φH_2O is given by:

$$\varphi_{H2O} = (1 + 18X^{-1} + X^{-2})^{0.5} \quad \text{..... (7)}$$

Then, the Air Pressure Gradient Multiplier (Chisholm Equation) φair, is also given by:

$$\varphi_{air} = (1 + 18X^{-1} + X^{-2})^{0.5} \quad \text{..... (8)}$$

Finally, the Multiphase Pressure Gradient, $(\frac{\Delta P}{L})_{multi}$ can be found by the following equation:

$$\left(\frac{\Delta P}{L}\right)_{multi} = {\varphi_{H2O}}^2 * \left(\frac{\Delta P}{L}\right)_{H2O} = {\varphi_{air}}^2 * \left(\frac{\Delta P}{L}\right)_{air} \quad \text{..... (9)}$$

3.3 Moody Diagram

Using the Reynolds number from equation (3) and the Friction factor equation (4), the expected appropriate flow can be determined from the Moody diagram shown in figure 4.

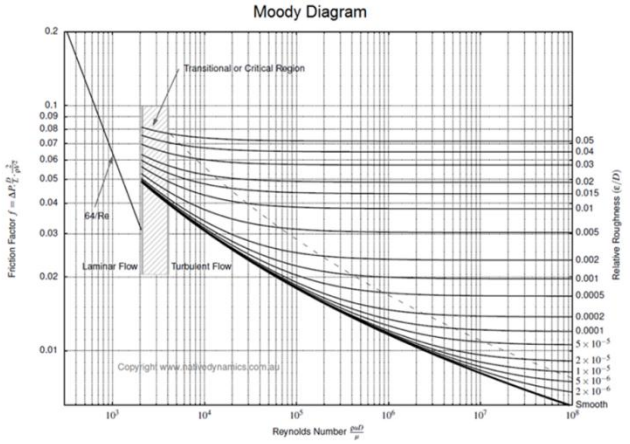

Figure 4: Moody Diagram: (Kleinstreuer C. Modern Fluid Dynamics. Springer, 2010)

From the moody diagram, we determined that from our Reynolds Number, Friction Factor, and Relative Roughness, we will experience Turbulent Flow.

IV. VERTICAL & INCLINED PIPE

ORIENTATION (BEGGS & BRILL CORRELATION)

The Beggs and Brill (1973) correlation are one of the few published correlations capable of handling all these flow directions. The correlation was developed by an experimental study of a two-phase flow in horizontal and inclined pipes. They designed a system of 1-inch and 1 ½-inch smooth circular pipes to investigate the inclination effect on liquid hold-up and pressure loss in gas and liquid two-phase flow (Beggs and Brill, 1973).

As a result of their experimental research, they produced the following correlation. Using this correlation, we calculated the pressure loss for our inclined and vertical sections, as depicted in our system diagram in figure 5a. The calculations are shown in Appendix B and C.

Calculate total flux rate

$$v_m = v_{sl} + v_{sg} \quad (10)$$

Calculate no-slip holdup

$$\lambda_{ns} = \frac{Vsl}{Vsl+Vsg} \quad (11)$$

Calculate the Froude number, NFR

$$N_{FR} = \frac{V_m 2}{gd} \quad (12)$$

$$N_{Lv} = V_{sl}\left(\frac{\rho l}{g\sigma_L}\right)^{0.25} \quad (13)$$

Calculate the correlating parameter, L_1, L_2, L_3 & L_4

$$L_1 = 316\lambda_{ns}^{0.302} \quad (14)$$

$$L_2 = 0.0009252\lambda_{ns}^{-2.4684} \quad (15)$$

$$L_3 = 0.10\lambda_{ns}^{-1.4516} \quad (16)$$

$$L_4 = 0.5\lambda_{ns}^{-6.738} \quad (17)$$

Determine the flow pattern using limits:

Segregated:

$$\lambda_{ns} < 0.01 \text{ and } N_{Fr} < L_1 \quad (18)$$

or

$$\lambda_{ns} \geq 0.01 \text{ and } N_{FR} < L_2 \quad (19)$$

Transition:

$$\lambda_{NS} \geq 0.01 \text{ and } L_2 < N_{FR} \leq L_3 \quad (20)$$

Intermittent:

$$0.01 \leq \lambda_{ns} < 0.4 \text{ and } L_3 < N_{Fr} \leq L_1 \quad (21)$$

or

Distributed:

$$\lambda_{ns} < 0.4 \text{ and } N_{FR} \geq L_1 \quad (22)$$

or

$$\lambda_{ns} \geq 0.4 \text{ and } N_{FR} > L_4 \quad (23)$$

Calculate the horizontal holdup λ_o

$$\lambda_o = \frac{a\lambda_{ns}^{b}}{N_{Fr}\, c} \quad (24)$$

The values for a, b, and c are determined for each flow pattern from table 1. These empirical coefficients are plugged into the equation to calculate the horizontal hold-up after determining the flow pattern. The value of a is multiplied by the no-slip hold up to the power of the b value. Froude's number is multiplied by the power of the c value (Maurer Engineering INC., 1994).

Table 1. Flow Pattern Coefficient

Flow Pattern	a	b	c
Segregated	0.98	0.4846	0.0868
Intermittent	0.845	0.5351	0.0173
Distributed	1.065	0.5824	0.0609

Calculate the inclination correction factor coefficient

$$C = (1-\lambda_{ns})\ln(d\lambda_{ns}^{e} N N_{Lv}{}^{f} N_{FR}{}^{g}) \quad (25)$$

The values for d, e, f, and g are determined for each flow condition from table 2. The values depend on the flow regime and direction, with the distributed uphill having no correction factor so that C will be zero giving ψ a value of one. The flow patterns have the same value for d, e, f, and g in the downhill direction. Interpolation should be performed if the flow is in the transition pattern (Maurer Engineering INC., 1994).

Table 2. Correction Factor Coefficient

Flow Pattern	d	e	f	g
Segregated uphill	0.011	-3.768	3.539	-1.614

Intermittent uphill	2.96	0.305	-0.4473	0.0978
Distributed uphill	No Correction		C = 0	
All flow patterns downhill	4.70	-0.3692	0.1244	-0.5056

Calculate the liquid holdup inclination correction factor

$$\psi = 1 + C[\sin(1.8\theta) - 0.333 \sin^3(1.8\theta) \quad (26)$$

Where θ is the deviation from horizontal axis.

Calculate the liquid hold-up.

$$\lambda = \lambda_o \psi \quad (27)$$

Apply Palmer Correction factor:

$$\lambda = 0.918 * \lambda \quad \text{for uphill flow} \quad (28)$$

$$\lambda = 0.541 * \lambda \quad \text{for downhill flow} \quad (29)$$

When flow is in a transition pattern, take the average as follows:

$$\lambda = a * \lambda_1 + (1 - a)\lambda_2 : \; a = \frac{L_3 - N_{Fr}}{L_3 - L_2} \quad (30)$$

Where λ_1 the liquid hold up calculated assuming the flow is segregated and λ_2 is the liquid holdup assuming the flow is intermittent.

Calculate the frictional factor ratio

$$\frac{f_{tp}}{f_{ns}} = e^s \quad (31)$$

Where,

$$S = \frac{\ln(y)}{-0.0523 + 3.182\ln(y) - 0.8725[ln(y)]^2 + 0.01853[\ln(y)]^4} \quad (32)$$

And $$y = \frac{\lambda_{ns}}{\lambda^2} \quad (33)$$

S becomes unbounded at a point in the interval 1 < y < 1.2; and for y in this interval, the function S is calculated from

$$S = \ln(2.2y - 1.2) \quad (34)$$

Calculate the frictional pressure gradient

$$(N_{Re})_{ns} = \rho_{ns} * v_m * de/\mu_{ns} \quad (35)$$

Use this no-slip Reynolds number to calculate no-slip friction factor, f_{ns} ‘, using Moody’s diagram, then convert it into Fanny friction factor $f_{ns} = f_{ns}$ ‘ /4.

The two-phase friction factor will be

$$f_{tp} = f_{ns} * \frac{f_{tp}}{f_{ns}} \quad (36)$$

The frictional pressure gradient is

$$\left(\frac{dp}{dx}\right)_f = \frac{2 f_{tp} \rho_{ns} * v_m^2}{d_e} \quad (37)$$

V. EXPERIMENTAL SETUP AND PROCEDURES

The experimental methods included the observation of flow regimes and the measuring of pressure differences. This was achieved by designing an undulating piping system that includes pipe orientations of horizontal, inclined, and vertical, as seen in the petroleum industry. An air compressor was used to create the effect of gas flowing through the pipe, while a water pump circulates water throughout the system. As shown in figure 5, the open channel system consists of sections 1.5 – 3 ft. long, 1 inch, and 1.5 diameter pipes installed in series emptying into a water tank. The system also consists of six pressure transducers installed before and after each experimental section of horizontal, vertical, and inclined orientations. Pressure gauges were also installed at the beginning and end of the system to monitor the overall pressure losses. In addition, figure 5b shows a flowmeter was installed before the air inlet to measure the flow rate of water by itself. The same was done with a pressure gauge to measure the air pressure. A Data Acquisition was installed on the back of the system board connected to a computer to record data from the pressure transducers. The electrical circuit of the DATAQ and pressure transducers is shown in figure 6.

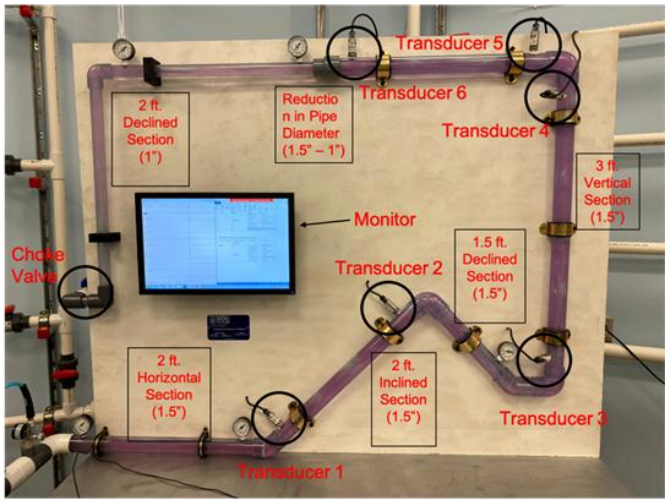

Figure 5. Experimental System, (a) Piping System

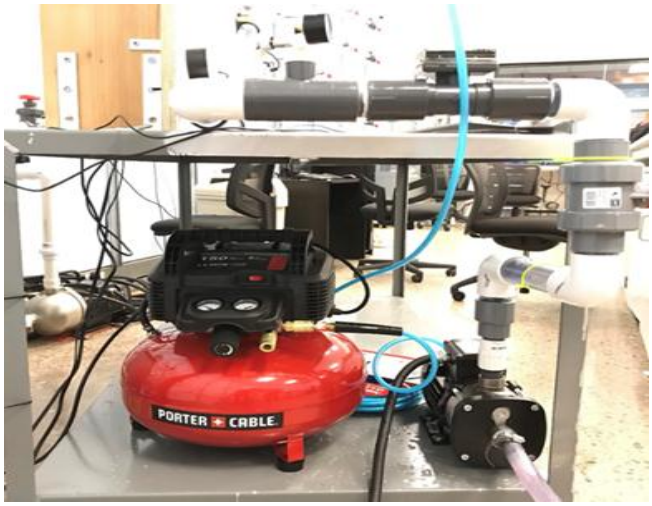

Figure 5., (b) Air Compressor & Water Pump.

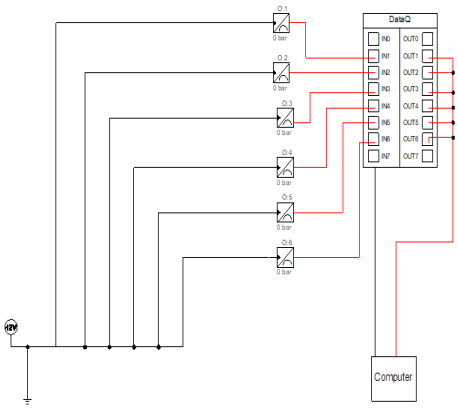

Figure 6 .DATAQ and Pressure Transducer Circuit

5.1. DATAQ Circuit

The circuit consists of six pressure transducers, each powered by a twelve-volt D.C supply. The transducers take the pressure readings and send them to the DATAQ logging instrument, which collects data. The DATAQ logging instrument is powered by the computer's CPU utilizing a USB, which transfers information between them. After the pressure readings are collected, it is sent to the computer to be interpreted using LabQuest.

5.2. Pipes & Fittings (Elbows)

Straight 1 and 1 ½ inch clear wall Schedule 80 PVC pipes were used for the experimental system. The pipes can withstand up to 200 psi at 72° F and a maximum of 140° F. The fittings used are 45° & 90°, 1 and 1 ½ inch Schedule 80 PVC elbows that are also able to withstand up to 200 psi 72° F and a maximum of 140° F. To connect the pipes and elbows, PVC primer and cement were used.

5.3. Water Pump

As shown in figure 3b, the water pump used in this experiment is a three-phase pump. It is compatible with a variable frequency drive, allowing water flow rate control. The variable frequency drive ranges from 0 – 60 Hz, where 60 Hz is equivalent to about 9.5 GPM.

5.4. Air Compressor

The air compressor, which is also shown in figure 3b, is the C2002, 6-Gallon, Oil-Free, Pancake Compressor. This pancake-style compressor is constructed this way for increased stability. The compressor also features a water drain valve and rigid rubber legs. The compressor delivers air at 40 psi of 3.5 SCFM and 90 psi 2.6 SCFM.

5.5. Procedure

A series of steps were carried out for the experimental work to be successful. The procedure of the experimental work is as follows:

1. Fill up the Water Tank and Pipe System with Water.
2. Turn on the Water Pump.
3. Turn on the Air Compressor.
4. Observe the flow regime through the different sections of the system.
   a. First, observe & record flow regime through the horizontal Pipe.
   b. Second, observe & record the flow regime through the inclined Pipe.
   c. Third, observe & record the flow regime through the vertical Pipe.
   d. Last, observe the flow regime through the smaller diameter pipe compared to the normal diameter pipe and note any difference.
5. Vary the Flowrates of water and air pressure to observe the differences in the four sections.
6. Report the different pressures at the gauges and pressure transducers.
7. Control choke valve to quarter, half, and three-quarter closed and record the influence on the pressure at the transducers.

VI. RESULTS/DISCUSSION

6.1. Chock Valve Positions Effect on System Pressure

Based on the theoretical calculations of pressure losses within our system, it was expected that the experimental pressure losses throughout the system would be minimal, which was proven. The main reason for the minimal loss and the low pressure of less than 2 psi within the system is an open system with an outlet pressure of 0 psi. There were minor pressure losses between the different sections and elbows. However, we increased the system pressure by small fractions by partially closing the choke valve at the outlet of the pipe circuit to quarter, half, and three-quarter closed. The reason for this specific experiment was to

increase our quantitative results by evaluating the effect of the choke valve at the end of the pipe circuit on system pressure at critical points. Figures 7 and 8 depict the pressure difference from transducers 1 through 6 (labeled in figure 5a) at different flow rates and air pressures for the four choke valve positions. These positions are open, quarter, half, and three-quarters closed. We chose 4 and 8 GPM flow rate because it includes both a flow rate and near maximum for our system. During observational experiments, we also saw greater variations in flow regime changes at these flow rates. Regarding our choice of air pressure, we experimented with air pressure from 10 psi through 120 psi. However, pressure differences were identical at 10 through 60 psi and 70 through 120 psi.

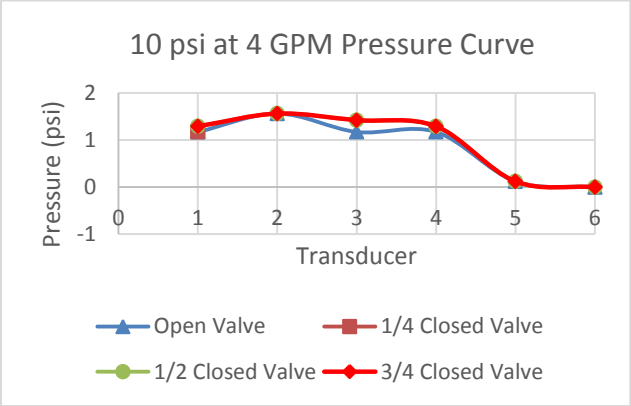

(a)

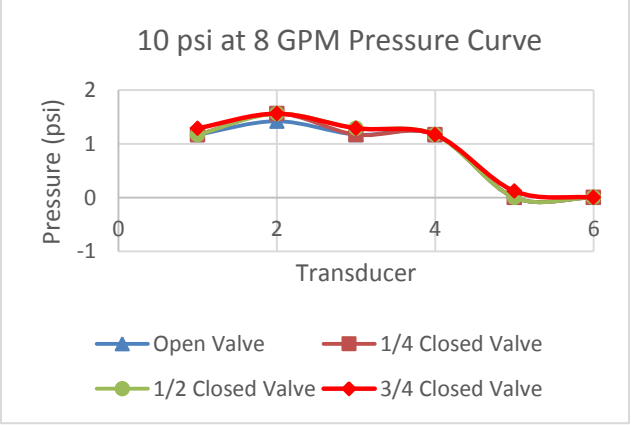

(b)

Figure 7.Pressure Curve (a) 10 psi Air-Pressure at 4 GPM, (b) 10 psi Air-Pressure at 8 GPM

Figure 7 compares pressure differences between a constant air pressure of 10 psi and differing water flow rates at 4 and 8 GPM influenced by the choke valve at the outlet of the system. As shown in figure 7a, closing the choke valve in three increments didn't significantly affect the system pressure recorded at the transducers until the valve was three-quarters closed. Though the initial pressure recorded at the first transducer and pressure at the fourth transducer were higher than all other choke valve positions, the greatest difference was at transducer three at the beginning of our 3-foot vertical section, where flow direction changes by 90º. In contrast with figure 7b, where the water flow rate is doubled, there were greater differences in pressure for each choke valve position. Transducer 1 records the same pressure for the open, quarter, and half-closed choke valve, while pressure is higher at transducer 2 for these positions. It is important to note that pressure is the same at transducer 4 for all choke positions, which indicates a 90º change in flow direction had no influence on system pressure in our system at low pressure.

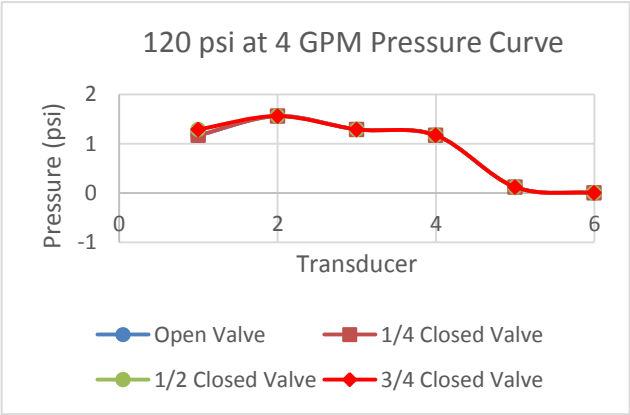

(a)

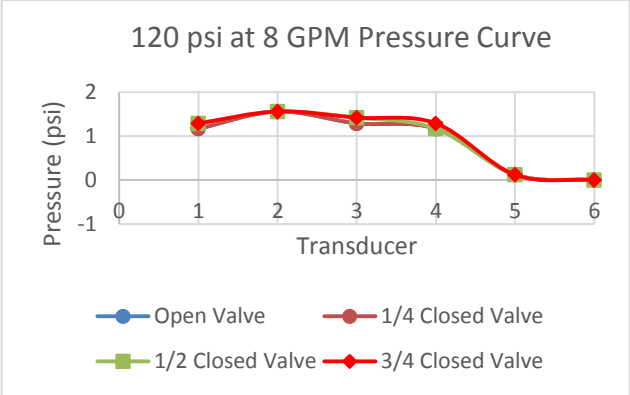

(b)

Figure 8. Pressure Curve (a) 120 psi Air-Pressure at 4 GPM, (b) 120 psi Air-Pressure at 8 GPM

Figure 8 also compares pressure differences between a constant air pressure of 120 psi and differing water flow rates at 4 and 8 GPM influenced by a chock valve at the outlet of the system. As shown in figure 8a, the closing of the choke valve in three increments didn't significantly affect the system pressure recorded at the transducers until the valve was three-quarters closed. However, this effect is considerably smaller at high air pressures when figure 8a is compared to figure 7a. The only impact closing the choke had on the recorded system pressure was at transducer one at three-quarter closed. The pressure remains the same for all positions at the different choke positions. Figure 8b of 120 psi at 8 GPM shows more variation of pressures for the different choke positions; however, they are minimal.

6.2. Effect of Air Pressure, Flow Rate & Pipe Orientation on Flow Regimes

Experimental results consist of observed flow regimes for vertical, horizontal, and inclined sections of the system. Air pressure varied in increments of 10psi to a maximum of 120 psi while the flow of water was kept constant and recorded in GPM. Figures 7 to 9 show the different flow regimes observed throughout the experiments.

Figure 9. Horizontal Section, (a) Stratified Flow

Figure 9., (b) Stratified Wavy Flow

Figure 7a shows stratified flow in the horizontal section of the experimental system. The system experienced stratified flow at a low water flow rate of 4 GPM up to 80 psi air pressure. Figure 7b shows stratified wavy flow in the same horizontal section as figure 7 of the experimental system. The system experienced stratified wavy flow at water flow rates above 4 GPM for air pressures under 90 psi and for flow rates 6, 8, and 9 GPM for air pressure 10 – 120 psi.

Figure 10. Vertical Section a) Bubble Flow b) Churn Flow c) Slug Flow

Figure 8a shows bubble flow in the vertical section of the experimental system. The system experienced this flow regime at a high-water flow rate of 9 GPM and low for air pressures under 40 psi. Figure 8 b shows churn flow in the same vertical section as figure 8a and 8c of the experimental system. This flow regime occurred at high experimented water flow rates and air pressures. Figure 8c shows slug flow in the same vertical section as figure 8b of the experimental system. This flow regime occurred at each experimented water flow rate but became more prevalent at higher air pressures.

Figure 11: Plug Flow in 45º Inclined Section

Figure 9 shows plug flow in the 45º inclined section of the experimental system. This flow regime occurred at each experimented water flow rate with low air pressure below 70 psi. The flow regimes observed in the system for the different flow rates of water and air was expected after previous theoretical calculation indicated turbulent flow using the Reynolds number from equation (3) and the Friction factor equation (4), then the Moody diagram. As shown in the images above and Appendix D, Stratified, Stratified Wavy, Bubble, Churn, Plug, and Slug Flow were observed. More specifically, in the horizontal section, Stratified Wavy Flow was observed throughout every

variation of flow velocity and air pressure except for 4 GPM water flow rates at air pressures less than 90 psi. In the vertical section, the flow regimes varied between Slug, Churn, and Bubble Flow, and for the inclined section, the flow regimes were predominately Plug and Slug Flow.

VII. CONCLUSION

Using the Lockhart-Martinelli Parameter coupled with the Chisholm Equation and the Beggs & Brill Correlation method, it was found that most of the pressure losses were in the elbows, and most frictional pressure loss occurred in the vertical 3ft pipe. In contrast, the 45° & 90° downhill pipes increased pressure. Comparisons were made between the theoretical and experimental results, and in both instances, it was found that most of the pressure loss occurred in the 45º and 90º elbows. The effect of the choke valve on pressure was also determined by comparing four choke valve positions of fully opened, ¼ closed. ½ closed and ¾ closed at six key locations of the system. These comparisons showed the closing of the choke valve in increments had more effect on system pressure at lower air pressure and flow rates than during high pressure and high flow rate environment and the most effect was at our third transducer where it was positioned at the beginning of our vertical 3 ft. pipe. As it relates to flow regimes, the flow regimes observed were generally what was expected given prior calculations that produced expected turbulent flow. Observed were churn flow, slug flow, plug flow, bubble flow, and stratified and stratified wavy flow, as shown in Appendix D tables. Specifically, in the horizontal section stratified flow was observed in horizontal section at low air pressures and water flow rates and stratified wavy flow higher flow velocities and air pressures. In the vertical section, the flow regimes varied between slug, bubble, and churn flow, and in the inclined section, the flow regimes also varied between slug and plug flow. Using the experimental system setup, we propose that future research can entail the effect of temperature on multiphase flow and the use of salt water or mineral oil.

REFERENCES

[1] Multiphase Flow in Oil and Gas Well Drilling, First Edition. Baojiang Sun. © 2016 Higher Education Press. All rights reserved. Published 2016 by John Wiley & Sons Singapore Pte. Ltd.

[2] Michaelides, E., & Feng, Z. (2016). Fundamentals of Multiphase Flow. In C. T. Crowe & J. D. Schwarzkopf (Eds.), Multiphase Flow Handbook, Second Edition (p. 1). Amsterdam University Press.

[3] Bai, Y., & Bai, Q. (2012). Multiphase Flow. In Subsea Engineering Handbook (1st ed., p. 371). Gulf Professional Publishing.

[4] Evaluation of Two-Phase Flow Characteristics in A Pipeline: Homogenous Model Approach, Okoye Obuora A, International Journal of Scientific & Technology Research Vol. 5, Issue 07, July 2016

[5] Alagorni, Abubaker & Yaacob, Z. & Nour, Abdurahman. (2015). An Overview of Oil Production Stages: Enhanced Oil Recovery Techniques and Nitrogen Injection. International Journal of Environmental Science and Development. 6. 693-701. 10.7763/IJESD.2015.V6.682.

[6] S. Corneliussen, J.-P. Couput, E. Dahl, E. Dykesteen, K.-E. Frøysa, E. Malde, H. Moestue, P. O. Moksnes, and L. Scheers nad H. Tunheim. Handbook of Multiphase Flow Metering. Norwegian Society for Oil and Gas Measurement, 2005.

[7] Griffith, Peter. "Multiphase Flow in Pipes." J Pet Technol 36 (1984): 361–367. doi: https://doi.org/10.2118/12895-PA

[8] Sarah, A., Julius, U., & Mary-Ann, O. (2014). Pressure Gradient Prediction of Multiphase Flow in Pipes. British Journal of Applied Science &Technology, 4(35), 4945–4958. https://doi.org/10.9734/bjast/2014/12985

[9] Orkiszewski, J.. "Predicting Two-Phase Pressure Drops in Vertical Pipe." J Pet Technol 19 (1967): 829–838. doi: https://doi.org/10.2118/1546-PA

[10] Fancher, G. H., & Brown, K. E. (1963, March 1). Prediction of Pressure Gradients for Multiphase Flow in Tubing. Society of Petroleum Engineers.doi:10.2118/440-PA

[11] Duns, H. and N. C. J. Ros. 1963. Vertical flow of gas and liquid mixtures in wells. In the 6th World Petroleum Congress. Frankfurt am Main, Germany: World Petroleum Congress.

[12] Hagedorn, Alton and Kermit Brown. 1965. "Experimental Study of Pressure Gradients Occurring During Continuous Two-Phase Flow in Small-Diameter Vertical Conduits." Journal of Petroleum Technology

[13] Beggs, D.H., and J.P. Brill. "A Study of Two-Phase Flow in Inclined Pipes." J Pet Technol 25 (1973): 607–617. doi: https://doi.org/10.2118/4007-PA

[14] J.H. Stuhmiller, The influence of interfacial pressure forces on the character of two-phase flow model equations, International Journal of Multiphase Flow, Volume 3, Issue 6, 1977, Pages 551-560, ISSN 0301-9322, https://doi.org/10.1016/0301-9322(77)90029-5.

[15] D.Z Zhang, A Prosperetti, Momentum and energy equations for disperse two-phase flows and their closure for dilute suspensions, International Journal of Multiphase Flow, Volume 23, Issue 3, 1997, Pages 425-453, ISSN 0301-9322, https://doi.org/10.1016/S0301-9322(96)00080-8.

[16] Taitel, Y, Bornea, D, and Dukler, A E. Modelling flow pattern transitions for steady upward gas-liquid flow in vertical tubes. [Bubble, slug, churn and dispersed-annular; also, existence regions and transitions]. United States: N. p., 1980. Web. doi:10.1002/aic.690260304

[17] Lockhart, R. W. and Martinelli, R. C., 1949, "Proposed Correlation of Data for Isothermal Two-Component Flow in Pipes", Chem. Eng. Prog., 45, pp. 39–48.

[18] Kutty, S.S., & Babu, T.A. (2017). Determination of Lockhart-Martinelli Parameter Using CFD in 2D Vertical Rectangular and offset Mini-Channels with R717.

[19] D. Chisholm, A theoretical basis for the Lockhart-Martinelli correlation for two-phase flow, International Journal of Heat and Mass Transfer, Volume 10, Issue 12, 1967, Pages 1767-1778, ISSN 0017-9310, https://doi.org/10.1016/0017-9310(67)90047-6.

[20] Kleinstreuer C. Modern Fluid Dynamics. Springer, 2010, ISBN 978-1-4020-8670-0

[21] Maurer Engineering INC. Multiphase Flow Production Model. January 1994.

NOMENCLATURE

f_{tp} = Two-phase friction factor

g = Gravitational acceleration (32.2 ft/ s2)

V_{sl} = Superficial liquid velocity (ft/s)

V_{sg} = Superficial gas velocity (ft/s)

V_m = Mixture velocity (ft/s)

Gpm = Gallons per Minute

psi = Pound per square inch

Ac= Cross-sectional area (m^2)

N_{Lv} = Calculate liquid velocity number

f_{H2O} = Friction factor water

f_{air} = Friction factor

f_{tp} = Two phase friction factor

$\left(\frac{dp}{dx}\right)_f$ =Frictional pressure gradient (psi)

j_{H2O} = Mass flux $(\frac{Kg}{sm^2})$

j_{air} = Find mass flux $(\frac{Kg}{sm^2})$

$\left(\frac{\Delta P}{L}\right)_{air}$ = Pressure gradient (Pa/m)

$\left(\frac{\Delta P}{L}\right)_{multi}$ = Pressure gradient (Pa/m)

$\left(\frac{\Delta P}{L}\right)_{H2O}$ = Pressure gradient $(Pa/m$

X = Lockhart-Martinelli parameter

d_e = Inner pipe diameter (mm)

Greek Symbols

λ_o = Horizontal holdup

λ = Palmer Correction factor

ψ = Liquid holdup inclination correction factor

φH_2O = Water pressure gradient multiplier

φ_{air} = Air pressure gradient multiplier

λ_{ns}= Calculate no-slip holdup

Dimensionless Group

N_{FR} = Froude number

R_{H2O}= Reynolds number (Pa/m)

R_{air} = Reynolds number, (Pa/m)

APPENDIX A

PRESSURE LOSS CALCULATION

HORIZONTAL SECTION

a. Find cross-sectional area, Ac

$$A_c = {D_H}^2$$

$$A_c = 0.0381^2$$

$$A_c = 0.00145\ m^2$$

b. Find mass flux, j_{H2O}

$$j = \frac{\dot{m}}{A_c}$$

$$j = \frac{0.95}{0.00145}$$

$$j = 654.45\frac{Kg}{sm^2}$$

c. Find Reynolds number, R_{H2O}

$$R_{H2O} = \frac{j * D_H}{\mu}$$

$$R_{H2O} = \frac{654.45 * .0381}{0.001002}$$

$$R_{H2O} = 24884.78$$

d. Find friction factor, f_{H2O}

$${f_{H2O}}^{-0.5} = -1.8log_{10}\left(\left(\frac{\frac{e}{D}}{3.7D_H}^{1.11}\right) + \left(\frac{6.9}{R_{H2O}}\right)\right)$$

$${f_{H2O}}^{-0.5} = -1.8log_{10}\left(\left(\frac{\frac{0.0000015}{3.7 * 0.0381}}^{1.11}\right) + \left(\frac{6.9}{24884.78}\right)\right)$$

$${f_{H2O}}^{-0.5} = 6.39$$

$$f_{H2O} = 0.0245$$

e. Find pressure gradient, $\left(\frac{\Delta P}{L}\right)_{H2O}$

$$\left(\frac{\Delta P}{L}\right)_{H2O} = \frac{f_{H2O} * (j_{H2O})^2}{2 * \rho_{H2O} * D_H}$$

$$\left(\frac{\Delta P}{L}\right)_{H2O} = \frac{0.0245 * (654.45)^2}{2 * 998.2 * 0.0381}$$

$$\left(\frac{\Delta P}{L}\right)_{H2O} = 137.96\frac{Pa}{m}\ /0.0200psi$$

Pressure Gradient for Air

Find cross-sectional area, A_c

$$A_c = {D_H}^2$$

$$A_c = 0.0381^2, \qquad A_c = 0.00145\ m^2$$

Find mass flux, j_{air}

$$j = \frac{\dot{m}}{A_c}$$

$$j = \frac{0.00143}{0.00145}$$

$$j = 0.99\frac{Kg}{sm^2}$$

Find Reynolds number, R_{air}

$$R_{air} = \frac{j * D_H}{\mu}$$

$$R_{air} = \frac{.99 * .0381}{1.983 * 10^{-5}}$$

$$R_{air} = 1902.12\frac{Pa}{m}\ /0.2759psi$$

Find friction factor, f_{air}

$${f_{air}}^{-0.5} = -1.8log_{10}\left(\left(\frac{\frac{e}{D}}{3.7D_H}^{1.11}\right) + \left(\frac{6.9}{R_{air}}\right)\right)$$

$$f_{air}{}^{-0.5} = -1.8log_{10}\left(\left(\frac{0.0000015}{3.7 * 0.0381}^{1.11}\right) + \left(\frac{6.9}{1902.12}\right)\right)$$

$$f_{air}{}^{-0.5} = 4.39$$

$$f_{air} = 0.0518$$

Find pressure gradient, $\left(\frac{\Delta P}{L}\right)_{air}$

$$\left(\frac{\Delta P}{L}\right)_{air} = \frac{f_{H2O} * (j_{air})^2}{2 * \rho_{air} * D_H}$$

$$\left(\frac{\Delta P}{L}\right)_{air} = \frac{0.0518 * (0.99)^2}{2 * 1.225 * 0.0381}$$

$$\left(\frac{\Delta P}{L}\right)_{air} = 0.264\frac{Pa}{m}/0.00003829psi$$

Lockhart-Martinelli Calculation

From the Pressure Gradient ($\frac{\Delta P}{L}$) the Lockhart-Martinelli parameter, X is given by:

$$\sqrt{\frac{\left(\frac{\Delta P}{L}\right)_{H2O}}{\left(\frac{\Delta P}{L}\right)_{air}}}$$

$$X = \sqrt{\frac{137.96}{0.264}}$$

$$X = 22.86$$

Total Multiphase Pressure Gradient

First the Water Pressure Gradient Multiplier (Chisholm Equation), φH_2O is given by:

$\varphi_{H2O} = (1 + 18X^{-1} + X^{-2})^{0.5}$

$\varphi_{H2O} = (1 + 1822.86^{-1} + 22.86^{-2})^{0.5}$

$\varphi_{H2O} = 1.338$

Then, the Air Pressure Gradient Multiplier (Chisholm Equation) $\varphi_{air,}$ is also given by:

$\varphi_{air} = (1 + 18X^{-1} + X^{-2})^{0.5}$

$\varphi_{air} = (1 + 1822.86^{-1} + 22.86^{-2})^{0.5}$

$\varphi_{air} = 1.338$

Finally, the Multiphase Pressure Gradient, $(\Delta P/L)_{multi}$ can be found by the following equation:

$$\left(\frac{\Delta P}{L}\right)_{multi} = \varphi_{H2O}{}^2 * \left(\frac{\Delta P}{L}\right)_{H2O} = \varphi_{air}{}^2 * \left(\frac{\Delta P}{L}\right)_{air}$$

$$\left(\frac{\Delta P}{L}\right)_{multi} = 1.338^2 * 137.96 + 1.338^2 * 0.264$$

$$\left(\frac{\Delta P}{L}\right)_{multi} = 247.45\ Pa/m/\ 0.03589psi$$

APPENDIX B

PRESSURE LOSS CALCULATION

VERTICAL SECTION

a.) Calculate total flux rate

$$v_m = v_{sl} + v_{sg}$$

$$v_m = 2.734 + 0.004$$

$$v_m = 2.74 \text{ ft/s}$$

b.) Calculate no-slip holdup

$$\lambda_{ns} = \frac{Vsl}{Vsl+Vsg}$$

$$\lambda_{ns} = \frac{2.734}{2.734+0.004}$$

$$\lambda_{ns} = 0.998$$

c.) Calculate the Froude number, NFR

$$N_{FR} = \frac{v_m 2}{gd}$$

$$N_{FR} = \frac{2.74^2}{4.036}$$

$$N_{FR} = 1.86$$

d.) Calculate liquid velocity number

$$N_{Lv} = V_{sl}(\frac{\rho l}{g\sigma_L})^{0.25}$$

$$N_{Lv} = 2.734(\frac{\rho l}{g\sigma_L})^{0.25}$$

e.) Calculate the correlating parameter L_1, L_2, L_3 & L_4

$$L_1 = 316\lambda_{ns}^{0.302}$$

$$L_1 = 316\lambda_{0.998}^{0.302}$$

$$L_1 = 315.86$$

$$L_2 = 0.0009252\lambda_{ns}^{-2.4684}$$

$$L_2 = 0.0009252\lambda_{0.998}^{-2.4684}$$

$$L_2 = 0.0009$$

$$L_3 = 0.10\lambda_{ns}^{-1.4516}$$

$$L_3 = 0.10\lambda_{0.998}^{-1.4516}$$

$$L_3 = 0.1002$$

$$L_4 = 0.5\lambda_{ns}^{-6.738}$$

$$L_4 = 0.5\lambda_{0.998}^{-6.738}$$

$$L_4 = 0.5051$$

Determine the flow pattern using limits:

Segregated:

$$\lambda_{ns} < 0.01 \text{ and } N_{Fr} < L_1$$

or

$$\lambda_{ns} \geq 0.01 \text{ and } N_{FR} < L_2$$

Transition:

$$\lambda_{NS} \geq 0.01 \text{ and } L_2 < N_{FR} \leq L_3$$

Intermittent:

$$0.01 \leq \lambda_{ns} < 0.4 \text{ and } L_3 < N_{Fr} \leq L_1$$

or

Distributed:

$$\lambda_{ns} < 0.4 \text{ and } N_{FR} \geq L_1$$

or

$$\lambda_{ns} \geq 0.4 \text{ and } N_{FR} > L_4$$

Calculate the horizontal holdup λ_o

$$\lambda_o = \frac{a\lambda_{ns}^{b}}{N_{Fr}^{c}}$$

$$\lambda_o = \frac{1.065\lambda_{0.998}^{0.5824}}{1.86_{0.0609}}$$

$$\lambda_o = 1.024$$

Where a, b, and c are determined for each flow pattern from the table 1:

Calculate the inclination correction factor coefficient

$$C = (1-\lambda_{ns})\ln(d\lambda_{ns}^{e}NN_{Lv}{}^{f}N_{FR}{}^{g})$$

Where d, e, f, and g are determined for each flow condition from the table 2:

Calculate the liquid holdup inclination correction factor

$$\psi = 1 + C[\sin(1.8\theta) - 0.333\sin^3(1.8\theta)]$$

$$\psi = 1 + 0[\sin(1.8 * 1.57) - 0.333\sin^3(1.8* 1.57)]$$

$$\psi = 1$$

Where θ is the deviation from horizontal axis.

Calculate the liquid hold-up.

$$\lambda = \lambda_o\psi$$

$$\lambda = 1.024 * 1$$

$$\lambda = 1.024$$

Apply Palmer Correction factor:

$$\lambda = 0.918 * \lambda \qquad \text{for uphill flow}$$

$$\lambda = 0.918 * 1.024$$

$$\lambda = 0.9400$$

$$\lambda = 0.541 * \lambda \qquad \text{for downhill flow}$$

$$\lambda = 0.541 * 1.024$$

$$\lambda = 0.5540$$

When flow is in transition pattern, take the average as follows:

$$\lambda = a * \lambda_1 + (1 - a)\lambda_2 : \; a = \frac{L_3 - N_{Fr}}{L_3 - L_2}$$

Where $\lambda_1$the liquid hold-up calculated assuming the flow is segregated and λ_2 is the liquid holdup assuming the flow is intermittent.

Calculate frictional factor ratio

$$\frac{f_{tp}}{f_{ns}} = e^{s}$$

$$\frac{f_{tp}}{f_{ns}} = e^{0.2339}$$

$$\frac{f_{tp}}{f_{ns}} = 1.2636$$

Where,

$$S = \frac{\ln(y)}{-0.0523 + 3.182\ln(y) - 0.8725[ln(y)]^2 + 0.01853[\ln(y)]^4}$$

$$S = \frac{\ln(0.9514)}{-0.0523 + 3.182\ln(0.9514) - 0.8725[ln(0.9514)]^2 + 0.01853[\ln(0.9514)]^4}$$

$$S = 0.2339$$

And $y = \frac{\lambda_{ns}}{\lambda^2}$

$$y = \frac{0.998}{1.024^2}$$

$$y = 0.9518$$

S becomes unbounded at a point in the interval 1 < y < 1.2; and for y in this interval, the function S is calculated from

$$S = \ln(2.2y - 1.2)$$

Calculate the frictional pressure gradient

$$(N_{Re})_{ns} = \rho_{ns} * v_m * de/\mu_{ns}$$

Use this no-slip Reynolds number to calculate no-slip friction factor, f_{ns}', using Moody's diagram, then convert it into Fanny friction factor $f_{ns} = f_{ns}'/4$.

The two-phase friction factor will be

$$f_{tp} = f_{ns} * \frac{f_{tp}}{f_{ns}}$$

$$f_{tp} = f_{ns} * \frac{f_{tp}}{f_{ns}}$$

$$f_{tp} = 0.0073 * 1.2636$$

$$f_{tp} = 0.009$$

The frictional pressure gradient is

$$\left(\frac{dp}{dx}\right)_f = \frac{2f_{tp}\,\rho_{ns} * v_m^2}{d_e}$$

$$\left(\frac{dp}{dx}\right)_f = \frac{2(0.009)\,(62.22)(2.74)^2(2.00)}{0.125*144*32.174}$$

$$\left(\frac{dp}{dx}\right)_f = 0.03 \text{ psi}$$

APPENDIX C

PRESSURE LOSS CALCULATION

INCLINED SECTION

a.) Calculate total flux rate

$$v_m = v_{sl} + v_{sg}$$

$$v_m = 2.734 + 0.004$$

$$v_m = 2.74 \text{ ft/s}$$

b.) Calculate no-slip holdup

$$\lambda_{ns} = \frac{Vsl}{Vsl+Vsg}$$

$$\lambda_{ns} = \frac{2.734}{2.734+0.004}$$

$$\lambda_{ns} = 0.998$$

c.) Calculate the Froude number, NFR

$$N_{FR} = \frac{v_m 2}{gd}$$

$$N_{FR} = \frac{2.74^2}{4.036}$$

$$N_{FR} = 1.86$$

d.) Calculate liquid velocity number

$$N_{Lv} = V_{sl}\left(\frac{\rho l}{g\sigma_L}\right)^{0.25}$$

$$N_{Lv} = 2.734\left(\frac{\rho l}{g\sigma_L}\right)^{0.25}$$

e.) e.) Calculate the correlating parameter L_1, L_2, L_3 & L_4

$$L_1 = 316\lambda_{ns}^{0.302}$$

$$L_1 = 316\lambda_{0.998}^{0.302}$$

$$L_1 = 315.86$$

$$L_2 = 0.0009252\lambda_{ns}^{-2.4684}$$

$$L_2 = 0.0009252\lambda_{0.998}^{-2.4684}$$

$$L_2 = 0.0009$$

$$L_3 = 0.10\lambda_{ns}^{-1.4516}$$

$$L_3 = 0.10\lambda_{0.998}^{-1.4516}$$

$$L_3 = 0.1002$$

$$L_4 = 0.5\lambda_{ns}^{-6.738}$$

$$L_4 = 0.5\lambda_{0.998}^{-6.738}$$

$$L_4 = 0.5051$$

Determine the flow pattern using limits:

Segregated:

$$\lambda_{ns} < 0.01 \text{ and } N_{Fr} < L_1$$

or

$$\lambda_{ns} \geq 0.01 \text{ and } N_{FR} < L_2$$

Transition:

$$\lambda_{NS} \geq 0.01 \text{ and } L_2 < N_{FR} \leq L_3$$

Intermittent:

$$0.01 \leq \lambda_{ns} < 0.4 \text{ and } L_3 < N_{Fr} \leq L_1$$

or

Distributed:

$$\lambda_{ns} < 0.4 \text{ and } N_{FR} \geq L_1$$

(22)

or

$$\lambda_{ns} \geq 0.4 \text{ and } N_{FR} > L_4$$

Calculate the horizontal holdup λ_o

$$\lambda_o = \frac{a\lambda_{ns}^{b}}{N_{Fr}^{c}}$$

$$\lambda_o = \frac{1.065\lambda_{0.998}^{0.5824}}{1.86_{0.0609}}$$

$$\lambda_o = 0.558$$

Where a, b, and c are determined for each flow pattern from the table 1:

Calculate the inclination correction factor coefficient

$$C = (1-\lambda_{ns})\ln(d\lambda_{ns}^{e}NN_{Lv}{}^{f}N_{FR}{}^{g})$$

$$C = 0$$

Where d, e, f, and g are determined for each flow condition from the table 2:
Calculate the liquid holdup inclination correction factor

$$\psi = 1 + C[\sin(1.8\theta) - 0.333\sin^3(1.8\theta)]$$

$$\psi = 1 + 0[\sin(1.8 * 1.57) - 0.333\sin^3(1.8 * 1.57)]$$

$$\psi = 1$$

Where θ is the deviation from horizontal axis.

Calculate the liquid hold-up.

$$\lambda = \lambda_o\psi$$

$$\lambda = 1.024 * 1$$

$$\lambda = 1.024$$

Apply Palmer Correction factor:

$$\lambda = 0.918 * \lambda \quad \text{for uphill flow}$$

$$\lambda = 0.918 * 1.024$$

$$\lambda = 0.9400$$

$$\lambda = 0.541 * \lambda \quad \text{for downhill flow}$$

$$\lambda = 0.541 * 1.024$$

$$\lambda = 0.5540$$

When flow is in transition pattern, take the average as follows:

$$\lambda = a * \lambda_1 + (1 - a)\lambda_2 : \; a = \frac{L_3 - N_{Fr}}{L_3 - L_2}$$

Where $\lambda_1$the liquid hold-up calculated assuming the flow is segregated and λ_2 is the liquid holdup assuming the flow is intermittent.

Calculate frictional factor ratio

$$\frac{f_{tp}}{f_{ns}} = e^{s}$$

$$\frac{f_{tp}}{f_{ns}} = e^{0.2339}$$

$$\frac{f_{tp}}{f_{ns}} = 1.2636$$

Where,

$$\mathbf{S} = \frac{\ln(y)}{-0.0523 + 3.182\ln(y) - 0.8725[ln(y)]^2 + 0.01853[\ln(y)]^4}$$

$$\mathbf{S} = \frac{\ln(0.9514)}{-0.0523 + 3.182\ln(0.9514) - 0.8725[ln(0.9514)]^2 + 0.01853[\ln(0.9514)]^4}$$

$$S = 0.2339$$

And $y = \frac{\lambda_{ns}}{\lambda^2}$

$$y = \frac{0.998}{1.0489}$$

$$y = 0.9514$$

S becomes unbounded at a point in the interval 1 < y < 1.2; and for y in this interval, the function S is calculated from

$$S = \ln(2.2y - 1.2)$$

Calculate the frictional pressure gradient

$$(N_{Re})_{ns} = \rho_{ns} * v_m * de/\mu_{ns}$$

Use this no-slip Reynolds number to calculate no-slip friction factor, f_{ns} , using Moody's diagram, then convert it into Fanny friction factor $f_{ns} = f_{ns}/4$.

The two-phase friction factor will be

$$f_{tp} = f_{ns} * \frac{f_{tp}}{f_{ns}}$$

$$f_{tp} = f_{ns} * \frac{f_{tp}}{f_{ns}}$$

$$f_{tp} = 0.0073 * 1.2636$$

$$f_{tp} = 0.009$$

The frictional pressure gradient is

$$\left(\frac{dp}{dx}\right)_f = \frac{2 f_{tp} \rho_{ns} * v_m^2}{d_e}$$

$$\left(\frac{dp}{dx}\right)_f = \frac{2(0.009)(62.22)(2.74)^2(3.00)}{0.125*144*32.174}$$

$$\left(\frac{dp}{dx}\right)_f = 0.04 \text{ psi}$$

APPENDIX D
Experimental FLOW REGIME Results

D1 – 10 psi at 4,6,8, and 9 GPM

Air Pressure (psi)	Water Flowrate (GPM)	Direction	Pattern
10	4	Horizontal	Stratified Flow
		Incline	Plug Flow
		Vertical	Churn Flow
	6	Horizontal	Stratified Wavy Flow
		Incline	Plug Flow
		Vertical	Churn Flow
	8	Horizontal	Stratified Wavy Flow
		Incline	Plug Flow
		Vertical	Churn Flow
	9	Horizontal	Stratified Wavy Flow
		Incline	Plug Flow
		Vertical	Bubble Flow

D2 - 20 psi at 4,6,8, and 9 GPM

Air Pressure (psi)	Water Flowrate (GPM)	Direction	Pattern
20	4	Horizontal	Stratified Flow
		Incline	Plug Flow
		Vertical	Slug Flow
	6	Horizontal	Stratified Wavy Flow
		Incline	Plug Flow
		Vertical	Churn Flow
	8	Horizontal	Stratified Wavy Flow
		Incline	Plug Flow
		Vertical	Churn Flow
	9	Horizontal	Stratified Flow
		Incline	Plug Flow
		Vertical	Bubble Flow

D3 – 30 psi at 4,6,8, and 9 GPM

Air Pressure (psi)	Water Flowrate (GPM)	Direction	Pattern
20	4	Horizontal	Stratified Flow
		Incline	Plug Flow
		Vertical	Slug Flow
	6	Horizontal	Stratified Wavy Flow
		Incline	Plug Flow
		Vertical	Churn Flow
	8	Horizontal	Stratified Wavy Flow
		Incline	Plug Flow
		Vertical	Churn Flow
	9	Horizontal	Stratified Flow
		Incline	Plug Flow
		Vertical	Bubble Flow

D4 - 40 psi at 4,6,8, and 9 GPM

Air Pressure (psi)	Water Flowrate (GPM)	Direction	Pattern
40	4	Horizontal	Stratified Flow
		Incline	Plug Flow
		Vertical	Slug Flow
	6	Horizontal	Stratified Wavy Flow
		Incline	Plug Flow
		Vertical	Slug Flow
	8	Horizontal	Stratified Wavy Flow
		Incline	Plug Flow
		Vertical	Slug Flow
	9	Horizontal	Stratified Wavy Flow
		Incline	Plug Flow
		Vertical	Slug Flow

D5- 50 psi at 4,6,8 and 9 GPM

Air Pressure (psi)	Water Flowrate (GPM)	Direction	Pattern
50	4	Horizontal	Stratified Flow
		Incline	Slug Flow
		Vertical	Slug Flow
	6	Horizontal	Stratified Wavy Flow
		Incline	Slug Flow
		Vertical	Slug Flow
	8	Horizontal	Stratified Wavy Flow
		Incline	Plug Flow
		Vertical	Slug Flow
	9	Horizontal	Stratified Wavy Flow
		Incline	Plug Flow
		Vertical	Slug Flow

D6 – 60 psi at 4,6,8 and 9 GPM

Air Pressure (psi)	Water Flowrate (GPM)	Direction	Pattern
60	4	Horizontal	Stratified Flow
		Incline	Slug Flow
		Vertical	Slug Flow
	6	Horizontal	Stratified Wavy Flow
		Incline	Slug Flow
		Vertical	Slug Flow
	8	Horizontal	Stratified Wavy Flow
		Incline	Plug Flow
		Vertical	Slug Flow
	9	Horizontal	Stratified Wavy Flow
		Incline	Slug Flow
		Vertical	Slug Flow

D7 – 70 psi at 4,6,8, and 9 GPM

Air Pressure (psi)	Water Flowrate (GPM)	Direction	Pattern
70	4	Horizontal	Stratified Flow
		Incline	Slug Flow
		Vertical	Slug Flow
	6	Horizontal	Stratified Wavy Flow
		Incline	Slug Flow
		Vertical	Slug Flow
	8	Horizontal	Stratified Wavy Flow
		Incline	Plug Flow
		Vertical	Slug Flow
	9	Horizontal	Stratified Wavy Flow
		Incline	Slug Flow
		Vertical	Slug Flow

D8 – 80 psi at 4,6,8 and 9 GPM

Air Pressure (psi)	Water Flowrate (GPM)	Direction	Pattern
80	4	Horizontal	Stratified Flow
		Incline	Slug Flow
		Vertical	Slug Flow
	6	Horizontal	Stratified Wavy Flow
		Incline	Slug Flow
		Vertical	Slug Flow
	8	Horizontal	Stratified Wavy Flow
		Incline	Plug Flow
		Vertical	Slug Flow
	9	Horizontal	Stratified Wavy Flow
		Incline	Slug Flow
		Vertical	Churn Flow

D9 – 90 psi at 4,6,8, and 9 GPM

Air Pressure (psi)	Water Flowrate (GPM)	Direction	Pattern
90	4	Horizontal	Stratified Wavy Flow
		Incline	Slug Flow
		Vertical	Slug Flow
	6	Horizontal	Stratified Wavy Flow
		Incline	Slug Flow
		Vertical	Slug Flow
	8	Horizontal	Stratified Wavy Flow
		Incline	Plug Flow
		Vertical	Slug Flow
	9	Horizontal	Stratified Wavy Flow
		Incline	Slug Flow
		Vertical	Churn Flow

D10 – 100 psi at 4,6,8, and 9 GPM

Air Pressure (psi)	Water Flowrate (GPM)	Direction	Pattern
100	4	Horizontal	Stratified Wavy Flow
		Incline	Slug Flow
		Vertical	Slug Flow
	6	Horizontal	Stratified Wavy Flow
		Incline	Slug Flow
		Vertical	Slug Flow
	8	Horizontal	Stratified Wavy Flow
		Incline	Plug Flow
		Vertical	Slug Flow
	9	Horizontal	Stratified Wavy Flow
		Incline	Slug Flow
		Vertical	Churn Flow

D11– 110 psi at 4,6,8, and 9 GPM

Air Pressure (psi)	Water Flowrate (GPM)	Direction	Pattern
110	4	Horizontal	Stratified Wavy Flow
		Incline	Slug Flow
		Vertical	Slug Flow
	6	Horizontal	Stratified Wavy Flow
		Incline	Slug Flow
		Vertical	Slug Flow
	8	Horizontal	Stratified Wavy Flow
		Incline	Plug Flow
		Vertical	Slug Flow
	9	Horizontal	Stratified Wavy Flow
		Incline	Slug Flow
		Vertical	Churn Flow

D12 – 120 psi at 4,6,8, and 9 GPM

Air Pressure (psi)	Water Flowrate (GPM)	Direction	Pattern
120	4	Horizontal	Stratified Wavy Flow
		Incline	Slug Flow
		Vertical	Slug Flow
	6	Horizontal	Stratified Wavy Flow
		Incline	Slug Flow
		Vertical	Slug Flow
	8	Horizontal	Stratified Wavy Flow
		Incline	Plug Flow
		Vertical	Slug Flow
	9	Horizontal	Stratified Wavy Flow
		Incline	Slug Flow
		Vertical	Churn Flow